The Conformational Ensemble of the β-Casein Phosphopeptide Reveals Two Independent Intrinsically Disordered Segments

Muhammad Ali Naqvi,[†] Sarah Rauscher,[‡] Régis Pomès,[§,∥] and Dérick Rousseau*[,†]

[†]Department of Chemistry and Biology, Ryerson University, Toronto, Ontario M5B 2K3, Canada
[‡]Max Plank Institute for Biophysical Chemistry, 37077 Göttingen, Germany
[§]Department of Biochemistry, University of Toronto, Toronto, Ontario M5S 1A8, Canada
[∥]Molecular Structure and Function, Hospital for Sick Children, Toronto, Ontario M5G 1X8, Canada

Ⓢ *Supporting Information*

ABSTRACT: The β-casein phosphopeptide 1−25 (βCPP) is involved in calcium binding, cellular transduction, and dental remineralization. Though the net charge of 13e suggests an intrinsically disordered peptide, it has been shown to possibly maintain partial structure. To investigate the nature and extent of its conformational disorder, 100 independent molecular dynamics simulations (cumulative time of 30 μs) were conducted in explicit water with 0.1 M sodium chloride. βCPP adopted an ensemble of conformations (R_g = 8.61 ± 0.06 Å) stabilized primarily by ionic interactions and less so by hydrogen bonding (HB). Intramolecular contact maps showed a lack of interaction between the peptide's head (RELEELNVPGEIVEΣ) and tail (ΣΣΣEESITR) segments, suggesting their conformational independence. While many backbone HB interactions were observed between the amino acids in each segment, there was no persistent secondary structure evident. Our findings provide a framework for further investigation of βCPP's conformation and mechanism of action upon binding to calcium phosphate.
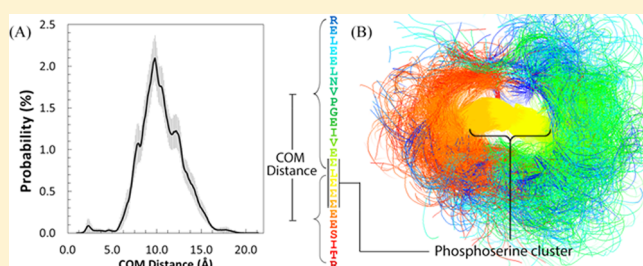
C asein phosphopeptides bind and increase the bioavailability of calcium phosphate (CaHPO₄) under various physiological conditions.[1] They are obtained from the tryptic digestion of the milk proteins α_{S1}-, α_{S2}-, and β-casein.[2] Given their capacity to improve calcium absorption and bioavailability, they have been shown to mitigate dental caries as well as oral diseases by hindering biofilm formation and favoring nucleation of apatitic CaHPO₄.[3,4] Their binding properties[5] and resilience against proteolysis[6] support their function as calcium carriers.

The β-casein phosphopeptide (βCPP) fragment (RELEEL-NVPGEIVEΣLΣΣΣEESITR) extends 25 amino acids from the N-terminus.[7] It contains four negatively charged phosphorylated serines (Σ) that electrostatically sequester calcium ions and promote the formation of calcium phosphate nanoclusters.[2,7,8] Once formed, the peptide−mineral complex becomes an effective vehicle for the efficient transport of CaHPO₄.[9,10] Ferraretto et al. showed that altering βCPP's primary sequence prevented calcium absorption, this inhibition being attributed to changes in conformation.[8] Some studies have claimed that the presence of secondary structure in βCPP is limited to only certain residues,[11] whereas others have stated that the entire peptide is completely disordered.[12] The secondary structure of βCPP has been extensively studied, albeit with little consensus (Table 1). However, its high net charge density per residue (0.52) and the prevalence of glutamic acid residues[13] strongly suggest that βCPP is an intrinsically disordered peptide (IDP).[14,15]

IDPs are defined by their conformational ensembles, which are a set of spatial arrangements that the peptide chain can adopt. Experimental determination of such ensembles is difficult because of averaging and data set bias. Since IDPs can adopt multiple conformations, structural studies yield an average of the entire ensemble in which salient features are lost.[13]

Computer simulations are not limited by such experimental constraints and can provide not only atomic resolution of IDPs but also insight regarding their conformational ensemble.[32] The first energy-minimized structure of β-casein by Kumosinski[28] provided evidence of a tendency toward bends in the N-terminus of the protein.[28] Farrell et al.[11] performed a 200 ps explicit solvent simulation of βCPP and found that a significant number of its amino acids were involved in bends.[11] Yasar et al.[31] identified three segments of β-casein [f(1−6, 35−40, and 43−48)] that maintained helical conformations consistent with Kumosinski's model.[28,31]

Though these simulations provided insight into βCPP's conformation, their length was only in the picosecond range. The minimal amount of time required for the equilibrium folding of a 25-residue peptide is predicted to be ∼250 ns.[33]

Table 1. DSSP Representation of βCPP Secondary Structure[c]

(G: 3₁₀, H: α, I: π) helix, B: β-bridge, E: Extended OR β-sheet, T: Turn, S: Bend, L: Loop, P: PPII Helix

1°		Technique	Reference	Year
	10| 20| RELEELNVPGEIVEΣLΣΣΣEESITR			
2°	HHHH HHHHHH	CD+CF,GR,RP,SE,WK	*[22, 23]	1975/81
	TTTTEEEE TTTTTT	CD+CF,VIL	*[24]	1984
	~~HHHH~~ HHHHHHH	CD[a]	[25]	1988
	HH	CF	*[26]	1987
	TTTT	NMR[b]	[27]	1991
	S S SSSSS S	In vacuo EM	*[28]	1993
	EEEE EEEEE	NMR	[29]	1993
	LLLL TTTT TTTTTTTT	NMR	[30]	2001
	P P P PPPP P P	CF		
	EE E E EEEEEEEEEE E EH	Chemical Shift	[11]	2002
	EE H E EEEEE H	NMR Shifts		
	S S S SS SS SGGG	MD		
	HHHH	>10% Probability	[31]	2006
	TTTT	In vacuo MD		

[a]Strikethrough indicates the absence of the specified structure. An asterisk indicates structure based on the entire β-casein protein. Helix formation observed in >40% 2,2,2-trifluoroethanol. [b]Type II β turn propensity, but not all connections were found. [c]Experimental methods: CD, circular dichroism; NMR, nuclear magnetic resonance. Sequence-based prediction methods: CF, Chou−Fasman;[16] GR, Garnier, Osguthorpe, and Robson;[17] RP, Robson and Pain;[18] SE, Schiffer and Edmundson;[19] VIL, Lim VI;[20] WK, Wu and Kabat.[21] Theoretical methods: EM, energy minimization; MD, molecular dynamics.

Hence, these previous computational studies were too short to attain definitive structural data.

In this study, it was hypothesized that because of its high charge density per residue, prevalence of glutamic acid residues, and the lack of secondary structure consensus, βCPP is an IDP. Extensive molecular dynamics (MD) simulations (total simulation time of 30 μs) were performed (1) to examine whether βCPP is intrinsically disordered and (2) to localize and quantify the extent of disorder.

■ METHODS

Simulation Setup. An initial completely extended structure of βCPP[22] was generated through its primary sequence using Pymol (DeLano Scientific, http://www.pymol.org). The structure was modified to add phosphate groups with a net charge of 2e at the known loci of phosphorylation (amino acids 15 and 17−19).[34,35] The Protein Data Bank file was then imported into GROMACS 4.5.1[36] using the GROMOS 43a force field modified for phosphoserine groups.[37] This united-atom force field, which combines nonpolar hydrogen atoms with the heavy atoms to which they are covalently bound, was parametrized for protein simulations for all 20 common amino acids as well as their phosphorylated derivatives.[38] A dodecahedron box with a minimum edge-to-peptide distance of 14 Å was used as the simulation box to solvate the peptide with 3249 simple point charge (SPC) water molecules.[39] The high 13e charge was neutralized via the addition of 20 Na⁺ and 7 Cl⁻ counterions that ensured an ionic strength of ~0.1 M. After energy minimization through steepest descent and conjugate gradient in tandem, a 2 ps isothermal−isobaric (298 K, 1 atm) ensemble simulation using Langevin dynamics and Parinello−Rahman isotropic molecule-based scaling for pressure[40] was performed to ensure constant temperature and pressure. A position-restrained simulation in which the peptide was restrained by imposing an isotropic force penalty of 1000 N on all atoms was also performed for 10 ps to allow water to equilibrate locally around the peptide. For all simulations, the electrostatic interactions were evaluated by the particle mesh Ewald method[36] with a charge grid spacing of approximately 1.0 Å and cubic-spline interpolation, while Lennard-Jones interactions were evaluated using a 14.0 Å cutoff.[36] The time step for the production run was 2 fs.

Simulations. One hundred independent simulations were conducted in parallel to minimize the effect of the initial conformation on equilibrium conformations. The initial starting structure of each replica was selected from a pool of 1000 different conformations obtained from 50 NVT 10 ns simulations conducted at 1000 K with sampling every 0.5 ns. The backbone peptide bonds of all initial structures remained in the $trans$ configuration. Each replica was simulated for 300 ns for a cumulative simulation time of 30 μs.

Analysis. The equilibration time for each simulation was determined by relative drift to the peptide's radius of gyration (R_g) at infinite time. This parameter was obtained using an exponential decay function $f(t)$ fit to the average of $R_g(t)$ over the 100 replicas. We defined equilibration time as the time required to reach $[|f(t) - f(\infty)|]/[f(\infty)] < 0.01$. This criterion was met within 100 ns, and therefore, the last 200 ns of each time trajectory was used for data analysis. Because there were 100 replicas, the cumulative simulation time used for the analysis was 20.0 μs. Simulation results were analyzed using the in-built tools provided with GROMACS.[41] Contact maps were generated by computing the fraction of time a specific pair of atoms was within a given distance. This distance cutoffs were determined using radial distribution functions. Polyproline II analysis was conducted using the method of Adzhubei et al.,[42] with an allowed deviation of ±20° from the ideal values of −75° and +145°.[42] This amount of deviation from ideal values is in agreement with a classification of PPII helices from globular proteins.[42]
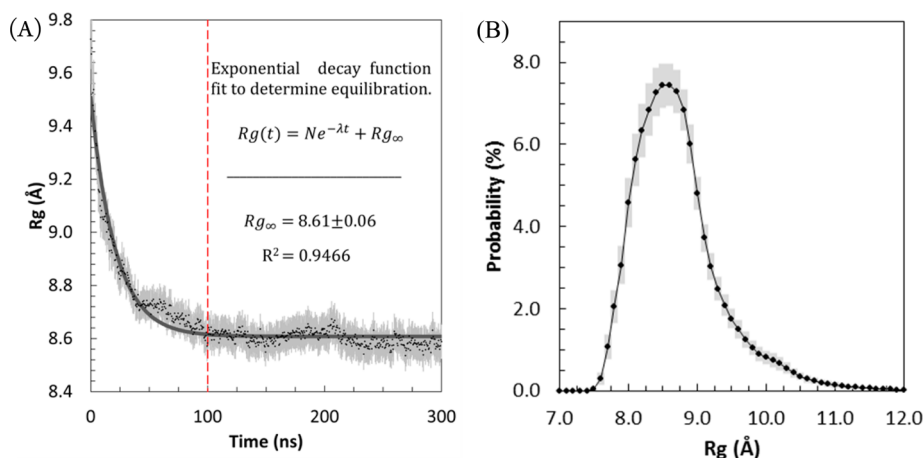
Figure 1. (A) Time evolution of the average R_g from 100 independent simulations. The dashed line shows the time at which the simulation was considered to be at equilibrium. (B) Average R_g probability distribution of βCPP from 100 to 300 ns. The standard error of the mean from 100 simulations is colored gray.

RESULTS AND DISCUSSION

Conformational Sampling. Our ultimate goal was to understand the conformational ensemble of βCPP. To evaluate the quality of the simulations, the number of possible intramolecular backbone hydrogen bonds (HBs) was used as a convergence metric as it is one of the slowest to equilibrate.[32] HBs were characterized by a distance cutoff r of ≤2.20 Å between the donor N−H and acceptor C=O groups. For any peptide of N amino acids and P prolines, the maximal number of backbone HBs that can be observed is

$$\text{Total no. of contacts} = N^2 - N - 2(N - 1) - NP \quad (1)$$

The first term N^2 represents the total number of permutations of HBs, whereas the second and third terms subtract the contacts of each amino acid with itself and with adjacent amino acids, respectively. Finally, the minus NP term accounts for the fact that the P prolines lack N−H groups. Hence, with 25 residues and one proline, 527 backbone HBs could theoretically occur within βCPP. The analysis of all simulation trajectories revealed that all 527 backbone HBs were sampled.

Peptide Equilibration. To assess peptide equilibration, we monitored the time evolution of the average R_g from the 100 simulations (Figure 1). The large initial average R_g value was due to the high temperature (1000 K) used to generate 100 uncorrelated starting conformations. The peptide collapsed into a stable conformational distribution within 100 ns (Figure 1A).

Analysis of the remaining 200 ns yielded an asymmetric R_g distribution with a peak probability at 8.60 ± 0.10 Å (Figure 1B), which was similar to the average $R_{g∞}$ using the exponential decay (8.61 ± 0.06 Å). Bioinformatics and polymer modeling data suggested that for a 25-amino acid random-coil peptide, the R_g would be ∼10 Å.[43,44] In our discussion below, we examine why the conformational ensemble of βCPP is relatively compact.

Overall Disorder. One simple way to test for disorder is through the Ramachandran map. Disordered peptides and proteins contain polyproline II (PPII) structures that are unstable in their conformation but have angles highly populated in the Ramachandran map ($φ ∼ -60°$, and $ψ ∼ 140°$).[45−47] βCPP exhibited a strong propensity for $φ$ and $ψ$ angles associated with the PPII structures (Figure 2), which compared favorably with past work on β-casein.[48] In a study that looked at
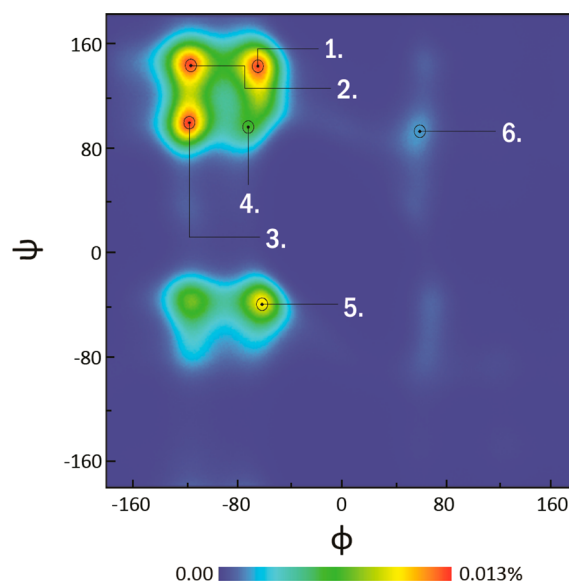

Figure 2. Ramachandran plot of dihedral angles for the replica simulation with assignments based on theoretical divisions: (1) polyproline II, (2) antiparallel β-sheet, (3) parallel β-sheet, (4) β-turn, (5) α-helix, and (6) left-handed helix.

the full β-casein molecule, Syme et al.[48] showed the presence of PPII structure using Raman optical activity.[48] Quantification of percent PPII structure within peptides and proteins can be done using the Ramachandran plot.[14,45−47] The percentage of PPII content predicted for βCPP using the Ramachandran angles was 11.9%. Farrell et al., who studied the peptide using circular dichroism, Fourier transform infrared, and primary structure predictions, indicated that up to 32% of the peptide could consist of PPII structure.[11]

The most common secondary structures present were turns, bends, and loops (Table 2). Given the lack of any higher-order secondary structures (i.e., helices and sheets) and the dominance of PPII angles in the Ramachandran map, these findings provided evidence that overall, βCPP is disordered.

Conformational Ensemble. Characterizing the conformational ensemble of IDPs requires quantifying all observed intramolecular interactions. One way to do so is by generating a contact map that quantifies the fraction of time a pairwise

Table 2. Secondary Structure Propensity within βCPP[a]

secondary structure	persistence (%)
3_{10}-helix $(i, i + 2)$	0.3
α-helix $(i, i + 3)$	0.8
π-helix $(i, i + 4)$	0.2
β-bridges	3.1
β-sheets	1.4
turns	15.9
bends	35.1
loops	43.2

[a]Loops are uncharacterized structures in the DSSP algorithm.

interaction between amino acids is encountered during the simulations. An interaction is defined as two atoms coming closer than a cutoff distance based on the radial distribution functions of those atoms. For nonpolar, HB, and ionic interactions, the selected atoms are backbone $C\alpha$, backbone N−H and C=O groups, and charged atoms in the peptide, respectively.

For $C\alpha$−$C\alpha$ distances and HB interaction, Figure 3A shows the nonpolar contacts observed during all βCPP simulations. All amino acids interacted with numerous partners as a result of conformational disorder. An interesting feature was the
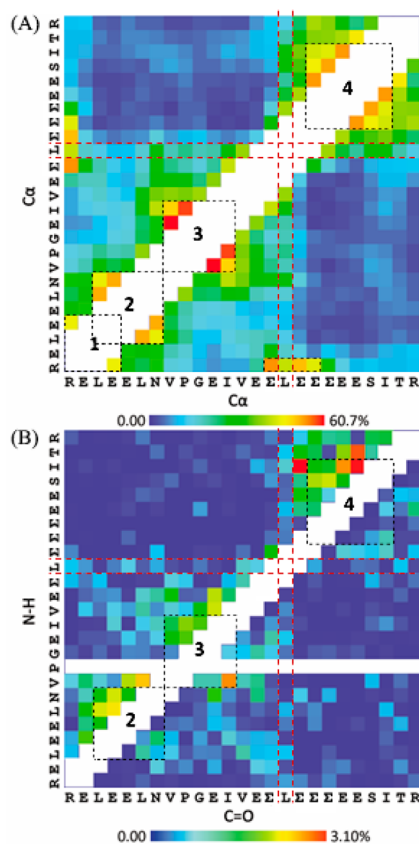

Figure 3. (A) Contact map based on a $C\alpha$−$C\alpha$ cutoff distance of 7.5 Å. Black dotted boxes indicate the most probable contacts. High-probability segments are shown in black boxes. (B) Hydrogen bond map showing possible intramolecular backbone interactions within βCPP. Dotted red lines show leucine 16, which delineates the head (bottom left) and tail (top right) segments of the peptide. Forward HBs are shown above the diagonal, while reverse HBs are shown below the diagonal. Color indicates percent probability. White segments denote removed HBs.

presence of two areas showing a lack of interaction (top left and bottom right). These two areas were equivalent because of the symmetry of the contact map and denoted preferential interactions between the head and tail ends of the peptide.

A completely disordered peptide will yield a contact map with similar probabilities for every possible interaction. By contrast, folded proteins yield maps with very high probabilities for a select few interactions. Figure 3A evokes the presence of two distinct segments in βCPP where contacts preferentially occur, the head [f1−15 (RELEELNVPGEIVEΣ)] and tail [f17−25 (ΣΣΣEESITR)] segments, which are linked by leucine 16. These segments, which are separated by the red dotted lines in Figure 3, show that all amino acids within each segment can interact with a number of other local residues along the peptide chain (e.g., E2 can associate with E4, E5, L6, etc.).

There were four groups of preferred local interactions along the peptide backbone: RELE (1), LEELN (2), VPGEI (3), and ΣΣEESI (4) (Figure 3A, dotted squares). The order of propensity for these interactions was as follows: VPGEI (60.7%) > ΣΣEESI (52.9%) > LEELN (51.4%) > RELE (45.1%). Interactions among groups 2−4 may be correlated with backbone interactions in the HB plot (Figure 3B), whereas group 1 was predominantly nonpolar as confirmed by its low probability in the HB and ionic bond map (Figure 4). A γ-turn (L6−V8) of low probability was also observed in the HB plot.
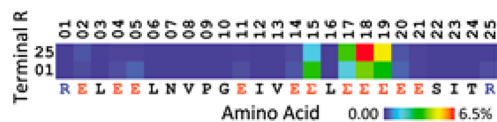

Figure 4. Propensity of ionic bond interactions between positive arginine side chains at the N- and C-termini and the negatively charged amino acids within βCPP. Color indicates percent probability relative to all possible ionic bonds during the simulation. The red amino acids are negatively charged, blue amino acids positively charged, and black amino acids neutral. Although all are shown for the sake of continuity, only charged residues were analyzed for probability.

The preference for forward (C=O$_i$···H−N$_j$, where $j > i$) over reverse (C=O$_i$···H−N$_j$, where $j < i$) hydrogen bonds reflected the stereochemistry of L-amino acids, which favor right-handed over left-handed conformations, respectively.[41,49] This preference was evident on the basis of the relatively smaller population of HBs to the bottom right of the diagonal on the contact map (Figure 3B). Interactions present along the diagonal of the HB map correspond to turns.[32] Groups 2 and 4 were associated with forward turns whereas group 3 was a reverse α-turn $(i, i − 4)$. The nonlocal interaction of R1 with ΣLΣΣ was mediated through ionic interactions (Figure 4). Although the existence of certain interactions in the peptide, notably VPGEI and ΣΣEESI, concurred with previous findings (Table 1), the results presented here clearly showed that these and every interaction in the peptide formed only some of the time.

Spatial Extension. Other than HB interactions, intramolecular ionic bonds also played a role in modulating the conformations of βCPP. Figure 4 plots the most probable ionic interactions present, with the terminal residues R1 and R25 shown on the y-axis and the primary sequence of the peptide on the x-axis. Of note, each terminal arginine interacted with the phosphoserine residues for a significant portion of the simulation time—17% for R25 and 12.8% for R1. R25 showed the highest probability of ionic bonding by associating with Σ18
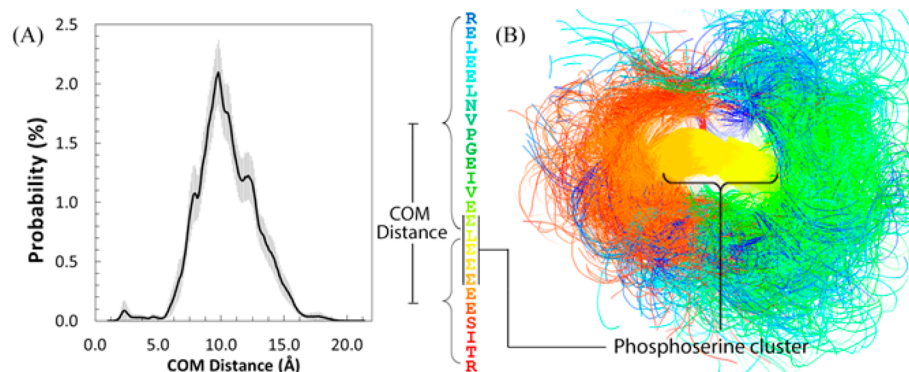
Figure 5. (A) Center of mass (COM) distance distribution between the head and tail segments showing their average separation distance. (B) Conformational diversity of βCPP. Alignment of 1972 conformations of the βCPP backbone obtained from equilibrium simulations. The peptide is colored from blue to red in rainbow colors from the N- to C-terminus, respectively, with the neck (leucine 16) colored yellow. The phosphoserine segment of amino acids 15−19 is outlined.

for 6.5% of the simulation time. By contrast, R1 interacted with Σ at positions 15 and 18 for 4.0% of the simulation time. Such a difference may be related to chain entropy as the greater R1-to-phosphoserine intervening sequence (13 and 6 for R1 and R25, respectively) reduced the probability of ionic bond formation.

Characterization of the Two Segments. The probability distribution of the distance between the head and tail segments showed a major peak at 9.8 ± 0.1 Å and minor peaks at 2.0, 7.8, and 11.6 Å (Figure 5A). The kurtosis of the distribution indicated that this was the prevailing separation distance between the two segments.

Figure 5B shows the combination of 1972 conformations aligned along residues 15−19, with the resulting compilation cropped to show the internal structure of the phosphoserine segment. The head and tail segments were distinct from one another and wrapped around the neck through backbone HB, as well as ionic interactions between amino acids. Because this was a superposition of conformations along the entire simulation trajectory, this figure also gives a sense of the space accessed by the structurally disordered βCPP.

On the basis of the nonpolar and HB maps, there was significant side-chain repulsion within the phosphoserine segment that resulted in a low probability of local backbone interactions (Figure 3A,B). The resulting stiffness of this segment was responsible for the physical separation of the head and tail segments of βCPP as well as their lack of interaction.

Comparison with the Literature. So far, only the VPGE turn in the βCPP sequence has been somewhat consistently predicted from sequence-based prediction algorithms[23,24] and experimentally through NMR[27,30] (Table 1). Although the Cα atoms of VPGE are within 7.5 Å for 60% of the simulation time (Figure 3A), the potential of forming a turn in this region is 3.1% (Figure 3B and Figure S5 of the Supporting Information). This confirms the results of Farrell et al.,[11] who found that a VPGE turn set in their initial structure did not persist through the molecular dynamics simulation.[11] The lack of VPGE turn probability is also in agreement with literature simulations on proline and glycine-rich peptides.[45] It has been found that glycine content is anticorrelated with turn formation as it increases the entropic cost of constraining the backbone.[45] It was also discovered that the loop in the initial segment RELE, which shows strong Cα−Cα interactions in Figure 3A, was similar to that found by Cross et al.[30] through NMR (Table 1).

Ferraretto et al. found that following transposition of the VPGE sequence with the initial RELE sequence, the influx of

Ca^{2+} ions into intestinal cells became minimal.[8] They speculated that these two sequences facilitated the transport of calcium through the cell membrane. In terms of functionality, the head and tail segments of βCPP have each been associated with separate functions in the literature. Ferraretto et al.[8] found that the tail end of βCPP was essential for Ca^{2+} binding while the head region was vital in promoting Ca^{2+} influx into intestinal cells.[8] Our discovery of these two distinct segments support the findings of Ferraretto et al.[8] and suggests that the exact primary sequence of βCPP has an important influence on the transport of calcium through cell membranes.

■ CONCLUSIONS

Despite its high net charge, βCPP is a relatively collapsed peptide with an R_g of 8.6 ± 0.1 Å. Interactions within the peptide are primarily nonpolar in nature, with ionic interactions being prevalent between the terminal arginines and phosphoseryl segment. The peptide is in a highly disordered state comprised of two independent, intrinsically disordered segments [head (RELEELNVPGEIVEΣ) and tail ($\Sigma\Sigma\Sigma$EESITR)] that are connected via leucine 16. Their independence is likely caused by electrostatic repulsion between the negatively charged side chains present in the neck segment. The discovery of these two independent segments may be linked to the dual functionality of βCPP previously reported in the literature.[8] In addition, 11.9% of the peptide conforms to the PPII structure, which is within the experimental limit. All of these structures and properties of βCPP must be viewed as working models with the flexibility to be changed as more precise data are obtained for βCPP. Future work will explore the binding conformation of this peptide in the presence of divalent cations.

■ ASSOCIATED CONTENT

ⓢ Supporting Information

Radial distribution functions for the determination of bond distance cutoffs, radii of gyration of head and tail segments, and the Ramachandran plot. This material is available free of charge via the Internet at http://pubs.acs.org.

■ AUTHOR INFORMATION

Corresponding Author
*E-mail: rousseau@ryerson.ca.

■ **REFERENCES**

(1) Cosentino, S., Donida, B. M., Marasco, E., Del Favero, E., Cantu, L., Lombardi, G., Colombini, A., Iametti, S., Valaperta, S., Fiorilli, A., Tettamanti, G., and Ferraretto, A. (2010) Calcium ions enclosed in casein phosphopeptide aggregates are directly involved in the mineral uptake by differentiated HT-29 cells. *Int. Dairy J. 20*, 770−776.

(2) Little, E. M., and Holt, C. (2004) An equilibrium thermodynamic model of the sequestration of calcium phosphate by casein phosphopeptides. *Eur. Biophys. J. 33*, 435−447.

(3) Cross, K. J., Huq, N. L., Palamara, J. E., Perich, J. W., and Reynolds, E. C. (2005) Physicochemical characterization of casein phosphopeptide-amorphous calcium phosphate nanocomplexes. *J. Biol. Chem. 280*, 15362−15369.

(4) Rahiotis, C., Vougiouklakis, G., and Eliades, G. (2008) Characterization of oral films formed in the presence of a CPP-ACP agent: An in situ study. *J. Dent. (Oxford, U.K.) 36*, 272−280.

(5) Holt, C., Sorensen, E. S., and Clegg, R. A. (2009) Role of calcium phosphate nanoclusters in the control of calcification. *FEBS J. 276*, 2308−2323.

(6) Boutrou, R., Coirre, E., Jardin, J., and Leonil, J. (2010) Phosphorylation and Coordination Bond of Mineral Inhibit the Hydrolysis of the β-Casein (1−25) Peptide by Intestinal Brush-Border Membrane Enzymes. *J. Agric. Food Chem. 58*, 7955−7961.

(7) Holt, C., Timmins, P. A., Errington, N., and Leaver, J. (1998) A core-shell model of calcium phosphate nanoclusters stabilized by β-casein phosphopeptides, derived from sedimentation equilibrium and small-angle X-ray and neutron-scattering measurements. *Eur. J. Biochem. 252*, 73−78.

(8) Ferraretto, A., Gravaghi, C., Fiorilli, A., and Tettamanti, G. (2003) Casein-derived bioactive phosphopeptides: Role of phosphorylation and primary structure in promoting calcium uptake by HT-29 tumor cells. *FEBS Lett. 551*, 92−98.

(9) Holt, C., Wahlgren, N. M., and Drakenberg, T. (1996) Ability of a β-casein phosphopeptide to modulate the precipitation of calcium phosphate by forming amorphous dicalcium phosphate nanoclusters. *Biochem. J. 314*, 1035−1039.

(10) Smyth, E., Clegg, R. A., and Holt, C. (2004) A biological perspective on the structure and function of caseins and casein micelles. *Int. J. Dairy Technol. 57*, 121−126.

(11) Farrell, H. M., Qi, P. X., Wickham, E. D., and Unruh, J. J. (2002) Secondary structural studies of bovine caseins: Structure and temperature dependence of β-casein phosphopeptide (1−25) as analyzed by circular dichroism, FTIR spectroscopy, and analytical ultracentrifugation. *J. Protein Chem. 21*, 307−321.

(12) Horne, D. S. (2002) Casein structure, self-assembly and gelation. *Curr. Opin. Colloid Interface Sci. 7*, 456−461.

(13) Rauscher, S., and Pomes, R. (2010) Molecular simulations of protein disorder. *Biochem. Cell Biol. 88*, 269−290.

(14) Mao, A. H., Crick, S. L., Vitalis, A., Chicoine, C. L., and Pappu, R. V. (2010) Net charge per residue modulates conformational ensembles of intrinsically disordered proteins. *Proc. Natl. Acad. Sci. U.S.A. 107*, 8183−8188.

(15) Uversky, V. N. (2011) Intrinsically disordered proteins from A to Z. *Int. J. Biochem. Cell Biol. 43*, 1090−1103.

(16) Chou, P. Y., and Fasman, G. D. (1978) Prediction of the secondary structure of proteins from their amino acid sequence. *Adv. Enzymol. 47*, 45−148.

(17) Garnier, J., Osguthorpe, D. J., and Robson, B. (1978) Analysis of accuracy and implications of simple methods for predicting secondary structure of globular proteins. *J. Mol. Biol. 120*, 97−120.

(18) Robson, B., and Pain, R. H. (1971) Analysis of code relating sequence to conformation in proteins: Possible implications for mechanism of formation of helical regions. *J. Mol. Biol. 58*, 237−257.

(19) Schiffer, M., and Edmundson, A. B. (1967) Use of helical wheels to represent structures of proteins and to identify segments with helical potential. *Biophys. J. 7*, 121−135.

(20) Lim, V. I. (1974) Algorithms for prediction of α-helical and b-structural regions in globular proteins. *J. Mol. Biol. 88*, 873−894.

(21) Kabat, E. A., and Wu, T. T. (1971) Attempts to locate complementarity-determining residues in variable positions of light and heavy-chains. *Ann. N.Y. Acad. Sci. 190*, 382−393.

(22) Creamer, L. K., Richardson, T., and Parry, D. A. D. (1981) Secondary Structure of Bovine α-S1-Casein and β-Casein in Solution. *Arch. Biochem. Biophys. 211*, 689−696.

(23) Bloomfield, V. A., and Mead, R. J. (1975) Structure and stability of casein micelles. *J. Dairy Sci. 58*, 592−601.

(24) Graham, E. R. B., Malcolm, G. N., and McKenzie, H. A. (1984) On the Isolation and Conformation of Bovine β-Casein-A-1. *Int. J. Biol. Macromol. 6*, 155−161.

(25) Chaplin, L. C., Clark, D. C., and Smith, L. J. (1988) The Secondary Structure of Peptides Derived from Caseins: A Circular-Dichroism Study. *Biochim. Biophys. Acta 956*, 162−172.

(26) Holt, C., and Sawyer, L. (1987) Predicted Secondary Structures in the Casein Family of Proteins. *Protein Eng. 1*, 243.

(27) Tsuda, S., Niki, R., Kuwata, T., Tanaka, I., and Hikichi, K. (1991) H-1-NMR Study of Casein Phosphopeptide (1−25): Assignment and Conformation. *Magn. Reson. Chem. 29*, 1097−1102.

(28) Kumosinski, T. F., Brown, E. M., and Farrell, H. M. (1993) 3-Dimensional Molecular Modeling of Bovine Caseins: An Energy Minimized β-Casein Structure. *J. Dairy Sci. 76*, 931−945.

(29) Wahlgren, N. M., Leonil, J., Dejmek, P., and Drakenberg, T. (1993) 2-Dimensional Nuclear-Magnetic-Resonance Study of the β-Casein Peptide 1−25: Resonance Assignments and Secondary Structure. *Biochim. Biophys. Acta 1202*, 121−128.

(30) Cross, K. J., Huq, N. L., Bicknell, W., and Reynolds, E. C. (2001) Cation-dependent structural features of β-casein-(1−25). *Biochem. J. 356*, 277−285.

(31) Yasar, F., Celik, S., and Koksel, H. (2006) The investigation of the secondary structures of various peptide sequences of β-casein by the multicanonical simulation method. *Phys. A (Amsterdam, Neth.) 363*, 348−358.

(32) Rauscher, S., and Pomès, R. (2010) Simulated tempering distributed replica sampling: A practical guide to enhanced conformational sampling. *J. Phys.: Conf. Ser. 256*, 1−13.

(33) Kubelka, J., Hofrichter, J., and Eaton, W. A. (2004) The protein folding 'speed limit'. *Curr. Opin. Struct. Biol. 14*, 76−88.

(34) Farrell, H. M., Jimenez-Flores, R., Bleck, G. T., Brown, E. M., Butler, J. E., Creamer, L. K., Hicks, C. L., Hollar, C. M., Ng-Kwai-Hang, K. F., and Swaisgood, H. E. (2004) Nomenclature of the proteins of cows' milk: Sixth revision. *J. Dairy Sci. 87*, 1641−1674.

(35) Sawyer, L., and Holt, C. (1993) The Secondary Structure of Milk-Proteins and Their Biological Function. *J. Dairy Sci.* 76, 3062−3078.

(36) Hess, B., Kutzner, C., van der Spoel, D., and Lindahl, E. (2008) GROMACS 4: Algorithms for highly efficient, load-balanced, and scalable molecular simulation. *J. Chem. Theory Comput.* 4, 435−447.

(37) Smith, G. (2009) *G43a1 forcefield modified to contain SEP (phosphoserine), TPO (phosphothreonine), and PTR (phosphotyrosine).* http://www.gromacs.org/Downloads/User_contributions/Force_fields.

(38) Wu, W., Kerrigan, J. E., Yadav, P., Schwartz, B., Izotova, L., Lavoie, T. B., and Pestka, S. (2004) Design and construction of a phosphorylatable chimeric monoclonal antibody with a highly stable phosphate. *Oncol. Res.* 14, 541−558.

(39) Scott, W. R. P., Hunenberger, P. H., Tironi, I. G., Mark, A. E., Billeter, S. R., Fennen, J., Torda, A. E., Huber, T., Kruger, P., and van Gunsteren, W. F. (1999) The GROMOS biomolecular simulation program package. *J. Phys. Chem. A* 103, 3596−3607.

(40) Berendsen, H. J. C., Postma, J. P. M., Vangunsteren, W. F., Dinola, A., and Haak, J. R. (1984) Molecular dynamics with coupling to an external bath. *J. Chem. Phys.* 81, 3684−3690.

(41) Kabsch, W., and Sander, C. (1983) Dictionary of Protein Secondary Structure: Pattern Recognition of Hydrogen-Bonded and Geometrical Features. *Biopolymers* 22, 2577−2637.

(42) Adzhubei, A. A., and Sternberg, M. J. E. (1993) Left-Handed Polyproline-II Helices Commonly Occur in Globular Proteins. *J. Mol. Biol.* 229, 472−493.

(43) Narang, P., Bhushan, K., Bose, S., and Jayaram, B. (2005) A computational pathway for bracketing native-like structures for small α helical globular proteins. *Phys. Chem. Chem. Phys.* 7, 2364−2375.

(44) Kohn, J. E., Millett, I. S., Jacob, J., Zagrovic, B., Dillon, T. M., Cingel, N., Dothager, R. S., Seifert, S., Thiyagarajan, P., Sosnick, T. R., Hasan, M. Z., Pande, V. S., Ruczinski, I., Doniach, S., and Plaxco, K. W. (2004) Random-coil behavior and the dimensions of chemically unfolded proteins. *Proc. Natl. Acad. Sci. U.S.A.* 101, 12491−12496.

(45) Rauscher, S., Baud, S., Miao, M., Keeley, F. W., and Pomes, R. (2006) Proline and glycine control protein self-organization into elastomeric or amyloid fibrils. *Structure* 14, 1667−1676.

(46) Shi, Z. S., Olson, C. A., Rose, G. D., Baldwin, R. L., and Kallenbach, N. R. (2002) Polyproline II structure in a sequence of seven alanine residues. *Proc. Natl. Acad. Sci. U.S.A.* 99, 9190−9195.

(47) Zagrovic, B., Lipfert, J., Sorin, E. J., Millettt, I. S., van Gunsteren, W. F., Doniach, S., and Pande, V. S. (2005) Unusual compactness of a polyproline type II structure. *Proc. Natl. Acad. Sci. U.S.A.* 102, 11698−11703.

(48) Syme, C. D., Blanch, E. W., Holt, C., Jakes, R., Goedert, M., Hecht, L., and Barron, L. D. (2002) A Raman optical activity study of rheomorphism in caseins, synucleins and tau: New insight into the structure and behaviour of natively unfolded proteins. *Eur. J. Biochem.* 269, 148−156.

(49) Carter, P., Andersen, C. A. F., and Rost, B. (2003) DSSPcont: Continuous secondary structure assignments for proteins. *Nucleic Acids Res.* 31, 3293−3295.